Prediction value of IVIM Combining with BOLD-MRI in Diabetic Kidney Disease: A Prospective Cohort Study

Jing Li
Guangdong Provincial People's Hospital, Guangdong Academy of Medical Sciences
Yanhui Wang
Guangdong Provincial People's Hospital, Guangdong Academy of Medical Sciences
Xiaokai Mo
Guangdong Provincial People's Hospital, Guangdong Academy of Medical Sciences
Jianteng Xie
Guangdong Provincial People's Hospital, Guangdong Academy of Medical Sciences
Qiuling Li
Guangdong Provincial People's Hospital, Guangdong Academy of Medical Sciences
Sheng Li
Guangdong Provincial People's Hospital, Guangdong Academy of Medical Sciences
Chunfang Qi
Guangdong Provincial People's Hospital, Guangdong Academy of Medical Sciences
Tiantian Liang
Guangdong Provincial People's Hospital, Guangdong Academy of Medical Sciences
Yifan Zhang
Guangdong Provincial People's Hospital, Guangdong Academy of Medical Sciences
Shaogui Zhang
Guangdong Provincial People's Hospital, Guangdong Academy of Medical Sciences
Zujiao Chen
Guangdong Provincial People's Hospital, Guangdong Academy of Medical Sciences
Xueqian Qiu
Guangdong Provincial People's Hospital, Guangdong Academy of Medical Sciences
Shaochun Lin
Guangdong Provincial People's Hospital, Guangdong Academy of Medical Sciences
Shuting Zhang
Guangdong Provincial People's Hospital, Guangdong Academy of Medical Sciences
Li Zhang
Guangdong Provincial People's Hospital, Guangdong Academy of Medical Sciences
Ting Lin

Guangdong Provincial People's Hospital, Guangdong Academy of Medical Sciences
Ruizhao Li
Guangdong Provincial People's Hospital, Guangdong Academy of Medical Sciences
Zhilian Li
Guangdong Provincial People's Hospital, Guangdong Academy of Medical Sciences
Xinling Liang
Guangdong Provincial People's Hospital, Guangdong Academy of Medical Sciences
Zhongwen Li
Guangdong Provincial People's Hospital, Guangdong Academy of Medical Sciences
Hongmei Chen
Guangdong Provincial People's Hospital, Guangdong Academy of Medical Sciences
Jian Kuang
Guangdong Provincial People's Hospital, Guangdong Academy of Medical Sciences
Zaiyi Liu
Guangdong Provincial People's Hospital, Guangdong Academy of Medical Sciences
Shuixing Zhang
Guangdong Provincial People's Hospital, Guangdong Academy of Medical Sciences
Wenjian Wang (wwjph@126.com)
Guangdong Provincial People's Hospital, Guangdong Academy of Medical Sciences

---

Research Article

Keywords: blood oxygen level-dependent (BOLD), diabetic kidney disease (DKD), intravoxel incoherent motion (IVIM), outcomes, twelve-layer concentric objects (TLCO)

Posted Date: December 23rd, 2020

DOI: https://doi.org/10.21203/rs.3.rs-122314/v1

Abstract

Background Noninvasive evaluation of hypoxia and fibrosis in kidney simultaneously by functional magnetic resonance imaging (MRI) to predict the prognosis of patients in prospective diabetic kidney disease (DKD) cohort has not been reported. We aim to assess the prediction value of blood oxygen level-dependent (BOLD) MRI and intravoxel incoherent motion (IVIM) diffusion-weighted image (DWI) in the prognosis of DKD.

Methods 77 patients with diabetes mellitus (67 with DKD) were enrolled in this prospective cohort study in single center. BOLD-MRI and IVIM-DWI were used to assess renal hypoxia and fibrosis. A well-validated, reproducible method called twelve-layer concentric objects (TLCO) was applied to quantify the R2* values of BOLD (corresponds to oxygenation) and D values of IVIM (corresponds to fibrosis) derived from MRI. All patients received standard medical care according to guideline during study and followed up for 24.8 ± 12.6 months. The primary end points were serum creatinine (Scr) increasing > 30%, ERSD, or death.

Results Our data demonstrated that medullary R2* value (MR2*) was significantly higher and cortical D value (CD) was markedly lower in DKD than those of diabetic controls, and strongly correlated with estimated glomerular filtration rate. Both the higher MR2* (log-rank test, $P < 0.001$) and the lower CD (log-rank test, $P < 0.001$) predicted a worse outcome of DKD. The corresponding areas under the curve (AUC) were 0.80 [95% confidence interval (CI) 0.69–0.89] and 0.77 (95% CI 0.64–0.89) respectively. Importantly, combination of MR2* and CD exhibited a more significant efficiency (AUC 0.85, 95% CI 0.74–0.95) than each of them respectively in predicting the outcomes of DKD.

Conclusions Integrating BOLD-MRI and IVIM-DWI quantified by TLCO was more efficient than each single of them in assessment of renal outcomes; thus, could be a noninvasive tool to predict the prognosis of DKD.

Trial registration The study protocol was registered at the Chinese Clinical Trial Registry Center (NO: ChiCTR-RRC-17012687; date of registration: 16/09/2017).

Background

Renal ischemia and fibrosis, the main pathological characteristics/features of progressive diabetic kidney disease (DKD) due to tubulointerstitial and vascular injury, contribute to the development of DKD [1–4]. Accurate and non-invasive evaluation of these factors would be helpful to predict the outcome of DKD. Although the measurement of renal parenchymal fibrosis and hypoxia in vivo remains challenging, the technological progress of functional magnetic resonance imaging (fMRI) makes it possible in clinical practice.

Blood oxygen level-dependent (BOLD) MRI measures renal tissue deoxyhaemoglobin levels voxel by voxel. Increases in its outcome measure R2* (transverse relaxation rate expressed as per second) correspond to higher deoxyhaemoglobin concentrations and suggest lower oxygenation, whereas

decreases in R2* indicate higher oxygenation [5]. BOLD-MRI monitors tissue oxygenation with deoxyhaemoglobin as an endogenous biomarker [6]. A linear relationship between directly measured renal pO_2 and R2* value has been validated in animal studies, which confirms that the measurement of hypoxia in tissue by BOLD is reliable [7, 8]. Some studies in human have also confirmed the feasibility of BOLD for evaluating renal injury in CKD with [9] or without diabetes [10]. Encouragingly, cortical R2* value may be used as a potential parameter for predicting renal function decline for patients with CKD according to recent studies [11, 12].

Diffusion-weighted magnetic resonance imaging (DWI) is a promising non-invasive method and sensitive to local water motion in the tissue; it is the technology to capitalize on the different diffusion features of fibrotic and nonfibrotic tissue [13, 14]. Common metric apparent diffusion coefficient (ADC) summarizes water diffusivity and flowing occurring in the kidney. The change of ADC may relate to the process of renal fibrogenesis [15], for it has been reported that ADC is significantly lower in CKD patients than health controls [10, 16]. A new procedure named intravoxel incoherent motion (IVIM) [10, 17], which is capable to separate D value (the true water diffusion coefficient in the tissue) and D* value (the pseudo diffusion) respectively, is invented recognizing that ADC is inevitably influenced by perfusion factors. In particular, D value reflects variations of intercellular water movement which is restricted mainly by interstitial fibrosis [18], and is used to assess renal fibrosis [19–21]. Recently, the clinical application of BOLD or IVIM in evaluation of renal function have been noticed [9, 11, 22].

Although short-term or cross-section studies have demonstrated that fMRI was helpful to evaluate the prognosis of CKD, prospective research to reveal the efficiency of integrating BOLD-MRI and IVIM-DWI for assessing the outcomes of DKD has not been reported.

Methods

Study Protocol

Patients

We screened 92 patients with diabetes mellitus (DM) in the division of nephrology and endocrinology of Guangdong Provincial People's Hospital from July 2014 to July 2016. 15 patients were excluded because that age > 70 years (n = 4), with renal cystic disease (n = 1), or unqualified imaging quality (n = 10).

DKD was defined as those diagnosed by pathological biopsy, or those with estimated glomerular filtration rate (eGFR) < 60 ml/min per 1.73 m^2, or presence of clinically detectable albuminuria over 3 months (24-hour albuminuria > 300 mg or albumin creatinine ratio > 300 mg/g) which was caused by diabetes [23]. Patient's baseline clinical characteristics were measured one week before fMRI examination.

Exclusion criteria: clinical data were incomplete; patient's age < 18 or > 70 years old; systolic pressure ≥ 180 mmHg or diastolic pressure ≥ 100 mmHg; patients with primary nephritis, hypertension, interstitial

nephritis, lupus, renal cyst disease, obstructive nephropathy, multiple renal calculi, or diameter of solitary renal cyst ≥ 30 mm.

Study execute

According to the definition of DKD above, 67 patients with kidney involved were defined as DKD group, while 10 patients without kidney involvement were selected as control (none-DKD group). All patients received BOLD-MRI and IVIM-DWI scanning at the base line and were followed up for at least 12months.

eGFR was calculated using Chronic Kidney Disease Epidemiology Collaboration (CKD-EPI) formula. Emission computed tomography-measured GFR (ECT-GFR) used plasma clearance of ^{99m}Tc-diethylenetriaminepentaacetic acid (^{99m}Tc-DTPA) was applied to evaluate GFR.

At least 6 hours before examination, all participants were instructed to stop taking diuretics, water and food. The other regular medications were continued following the guideline of KDOQI [23].

Primary outcome

The primary end points were defined as serum creatinine (Scr) increasing ≥ 30% [11] or end-stage renal disease (ESRD), or death. The end-time of follow-up was September 31, 2018. During follow-up period, all the patients received standard medical care according to guideline during study and were visited for every 6 months regularly. Patients lost contact were regarded as censored cases. The observation endpoint was reported to the principal investigator immediately with excluding acute state.

MRI acquisition

Measurements were carried out with a 3.0-T whole body MR scanner with an 8-channel body array coil for signal reception (Sigma EXCITE HD, GE Healthcare, Milwaukee, WI, USA). We used a respiratory triggering technique without breath-holding which many patients could not abide.

A multiple gradient-recalled-echo sequence was used for BOLD-MRI imaging. The parameters were listed as following: 100 ms repetition time; 3.8 ms echo time; 300 × 300 mm view field; 3.0 mm slice thickness; spacing between slices at 3.6 mm; 45° flip angle; 31.25 Hz/pixels band width; and 96 × 96 matrix. 5 coronal slices across the renal hilar vessels were acquired. Respiration trigger mode was adopted in image acquisition, total acquisition time was 5 minute and 18 seconds without breath-holding.

IVIM-DWI was performed with 10 diffusion gradient b values: 0, 20, 40, 60, 80, 100, 200, 400, 500 and 600 s per mm^2. Preset program was monoexponential. The following parameters were used for the sequence: 3000 ms repetition time; 60.6 ms echo time; 320 × 320 mm view field; 3.0 mm section thickness; spacing between slices at 3.6 mm; 90° flip angle; 1953 Hz/pixels band width; and 96 × 96 matrix size; 14 coronal slices across the renal hilar vessels were acquired. The entire acquisition time was 5 minute and 6 seconds by using respiration trigger mode.

MRI processing

The modified method of twelve layers concentric objects (TLCO) was implemented with Matlab 9.1.0 (The Math Works Inc, Natick, Massachusetts, USA), according to previously described [24]. On anatomic templates, the circumference of the renal parenchyma was drawn manually in the selected coronal slice. Following the previous study [24], we sketched the inner outline avoiding the portal vessels, and chose outer or inner 4 layers to analyze/for analysis. The selected renal parenchyma were divided into 12 layers with equal thickness called the concentric objects by an automatic algorithm, a set of pixels with a constant depth was covered for each object. The radial profile was obtained by the plotted curve of the value of each layer at increasing depth. Renal cortical values were calculated with the average value of the 4 outer layers, and medulla with 4 inner layers. Pseudo-color maps were built using graph analysis software (Function Tool 4.6, GE Healthcare Inc.).

Statistical analyses

Designed sample size was calculated by PASS version 11.0 (NCSS, Kaysville, Utah, USA), a minimum of 55 patients with DKD was needed to have 80% power to detect outcome variances, according previous study [11]. All statistical analysis was conducted by Prism 7.0 (GraphPad Software, San Diego, CA, USA). Quantitative values were expressed as mean ± SD. Normality was graphically assessed first, and then numerically with skewness and kurtosis test. Analysis of variance, unpaired samples *t* test and one-way *ANOVA* were used as appropriate to compare the clinical parameters and MRI datum. *Pearson* correlation coefficient was applied in the relationship analysis. Multivariable analysis of *Cox* regression was used to analyze the associations between the clinical outcomes and diversified variables. Receiver-operating characteristic (ROC) curve was built to compare the discriminative accuracy of different variables to assess the decline of renal function. Kaplan-Meier survival analysis was used to evaluate the difference of major renal events. A 2-tailed $P < 0.05$ was considered statistically significant.

Results

DKD patients exhibited higher R2* value and lower D value in kidney compared to DM control

As illustrated in Supplemental Fig. 1, 77 patients were enrolled in this prospective cohort study, and 10 patients lost contract. 67 patients were followed up and completed the experiment. Characteristics of subjects are summarized in Supplemental table 1. 24 patients reached the end points: 2 patients died (one of coronary heart disease; one of stroke); 18 patients reached ESRD; 4 patients demonstrated Scr-increase ≥ 30%. The average follow-up period (mean ± SD) was 24.6 ± 12.8 months. No significant difference in duration of DM, gender, BMI and age, was found between DKD and non-DKD group. However, patients with DKD presented markedly increase of albuminuria, serum creatinine, urea nitrogen, R2* values in medulla (MR2*) and cortex (CR2*) while significantly decrease of eGFR, ECT-GFR, and D values in cortex (CD) compared with non-DKD. These data indicated that patients with DKD exhibited prominent kidney damage with higher index of fibrosis (lower D value) and hypoxia (higher R2* value) compared to non-DKD.

As displayed in Supplemental table 2, variation coefficients of TLCO exhibited a lower inter-observer variability compared to method of regions of interest (ROI). Compared with non-DKD, patients with DKD exhibited a higher R2* profile ($P < 0.001$, Supplemental Fig. 2 g) and a lower D profile ($P < 0.01$, Supplemental Fig. 2 h) in renal parenchyma.

Pseudo-color maps of IVIM and BOLD were showed in Fig. 1a. We compared the values of cortex (4 outer layers) and medulla (4 inter layers) between DM and CKD 1–5 stages respectively. Profiles of D value were shown in Fig. 1b. D values in both cortex (CD) and in medulla (MD) at advanced DKD were markedly lower than those of non-DKD (Fig. 1c and 1d), potentially suggesting a higher fibrosis in DKD. Profiles of R2* in different groups were showed in Fig. 1e. R2* value in cortex (CR2*) and medulla (MR2*) in advanced DKD were significantly higher than those of non-DKD (Fig. 1f and 1 g), indicating higher hypoxia in DKD.

R2* and D values in kidney correlated to the renal function decline in DKD

We examined the correlations of R2* and D values with the baseline renal function represented by eGFR and ECT-GFR respectively. As depicted in Fig. 2, R2* values negatively correlated with eGFR (CR2*, $r = -0.58$, $P < 0.001$; MR2*, $r = -0.63$, $P < 0.001$) and ECT-GFR (CR2*, $r = -0.40$, $P < 0.01$; MR2*, $r = -0.51$, $P < 0.001$), indicating renal function inversely correlated with the level of oxygenation. However, D values positively correlated with eGFR (CD, $r = 0.50$, $P < 0.001$;MD, $r = 0.37$, $P < 0.01$), and ECT-GFR (CD, $r = 0.45$, $P < 0.001$; MD, $r = 0.28$, $P = 0.031$), prompting renal function positively correlated with the index of fibrosis. All the MRI values exhibited a better correlation with eGFR than ECT-GFR. MR2* and CD values were also better than CR2* and MD respectively. Our data suggested that fibrosis and hypoxia in the kidneys of DKD may be deteriorated by the decline of renal function.

MR2* and CD values predicted the outcomes of DKD

Because of the priority of MR2* and CD in the correlations with eGFR (indicated in Fig. 2), we further analyzed their associations with outcomes of DKD. Table 1 showed the results of multivariable regression analysis between the outcomes of DKD and the clinical independent variables, such as age, sex, baseline eGFR, albumin-creatinine ratio (ACR), hemoglobin (Hb), DM duration and use of medication. In age- and sex- adjusted models, the poor outcomes of DKD positively correlated with baseline eGFR (regression coefficient β: 0.94, 95% confidence interval [95% CI]: 0.92–0.97, $P = 0.001$), Hb (β: 0.95, [95% CI]: 0.92–0.98, $P = 0.004$), CR2* (β: 1.19, [95% CI]: 1.02–1.40, $P = 0.026$), MR2* (β: 1.14, [95% CI]: 0.99–1.31, $P = 0.045$), and CD (β: 0.89, [95% CI]: 0.81–0.98, $P = 0.020$), but not with other mentioned covariates. Those results suggested that a higher R2* value in renal parenchyma and a lower D value in cortex were signs of poor prognosis for DKD without the interference of age or gender. Our data did not exhibit a markedly association of duration of DM, ACR, and use of renin-angiotensin system blockers with the outcomes of DKD.

Table 1
Multivariable analysis of the associations between the outcomes of DKD and clinical variables.

	Age- and sex- adjusted β(95% CI)	*P* [a]
Age (yr)	0.98 (0.93 to 1.04)	0.146
Sex (female vs. male)	1.59 (0.53 to 5.04)	0.512
Baseline eGFR (ml/min per 1.73 m^2)	0.94 (0.92 to 0.97)	0.001
ACR (mg/g)	1.00 (1.00 to 1.001)	0.763
Hb (g/l)	0.95 (0.92 to 0.98)	0.004
DM duration (yr)	1.01 (0.93 to 1.10)	0.751
ACEI/ARB (yes vs.no)	0.49 (0.15 to 1.53)	0.931
Cortical R2* (s^{-1})	1.19 (1.02 to 1.40)	0.026
Medullary R2* (s^{-1})	1.14 (0.99 to 1.31)	0.045
Cortical D (mm^2/s)	0.89 (0.81 to 0.98)	0.020
Medullary D (mm^2/s)	0.92 (0.84 to 1.10)	0.106

[a]Adjusted for age, sex, baseline eGFR, ACR, Hb, DM duration and use of ACEI/ARB.

ACEI, angiotensin-converting enzyme inhibitor; ACR, albumin-creatinine ratio; ARB, angiotensin II receptor blocker; CI, confidence interval; DKD, diabetic kidney disease; DM, diabetes mellitus; eGFR, estimated glomerular filtration rate; Hb, hemoglobin.

To compare the outcomes of DKD different by the MRI variables, patients were stratified into 4 groups based on the interquartile range (IQR) of the MR2* and CD. Clinical characteristics according to MR2* or CD groups were provided in Supplemental table 3 and 4. The information of IQR groups based on MR2* or CD was summarized in Supplemental table 5. The information of IQR regroups based on the combination of MR2* and CD was summarized in Supplemental table 6. Kaplan-Meier survival shown that the higher MR2* (log-rank test, $P < 0.001$) and the lower CD (log-rank test, $P < 0.001$) predicted a worse outcome (Fig. 3a and 3c). The area under the curve (AUC) of MR2* (0.80, 95% CI 0.69–0.89) and the CD (0.77, 95% CI 0.64–0.89) showed the credible specificity and sensitivity to identify renal dysfunction respectively (Fig. 3b and 3d). Importantly, the Kaplan-Meier curve based on MR2* and CD combined was not only exhibited a significant log-rank (log-rank test, $P < 0.001$) (Fig. 3e), but also turned out to be the more significant AUC (0.85, 95% CI 0.74–0.95) than each one of them (Fig. 3f). ROC comparison confirmed that combination of MR2* and CD markedly increased the efficiency in prediction of the outcomes of DKD compared to each one of them respectively (Fig. 4).

Discussion

In current prospective cohort study, we indeed reveal that patients with DKD exhibited higher renal fibrosis (corresponding to lower D value) and worse hypoxia (corresponding to higher R2* value) compared to non-DKD, and the index of fibrosis (CD values) and hypoxia (MR2*) deteriorated by the decline of renal function. Further, either increased MR2* or decreased CD strongly correlated with poor outcomes of patients with DKD. Importantly, integrating MR2* and CD markedly increased the efficiency in assessment of DKD prognosis compared to each single of them respectively.

Accumulating evidence have emphasized the roles of renal tissue hypoxia and fibrosis [25, 26] in the progression of CKD regardless of etiology[27]. Although oxygen-sensitive microelectrodes could directly measure tissue oxygenation and the degree of fibrosis could be evaluated by biopsy, the highly invasive damage is the main obstacle in clinical practice [28]. Functional MRI is able to identify the signals of hypoxia and fibrosis in kidney simultaneously by the measurable translating values derived from fMRI images [29].

Our data demonstrated that the profile of R2* in DKD markedly increased compared to non-DKD, especially in advanced stages, which supported that renal hypoxia increased with progression in DKD (Fig. 1e and 1f). Higher R2* heralded a worse outcome (AUC was 0.80, as shown in Fig. 3b). Of note, part of patients were placed on long-term treatment of loop diuretics, for example, furosemide which inhibits sodium reabsorption, consequently, may decrease oxygen consumption[30, 31], because loop diuretics block the Na^+-K^+-$2Cl^-$ transporter in the thick ascending loop of Henle, and increase local pO_2 [32]. Besides, factors that affect the oxygen dissociation curve influence the BOLD-signal, such as body temperature, blood pH etc., make it inexact to predict prognosis with R2* value alone [33–36]. Thus, alternated method of fMRI called IVIM was applied in clinical practice recently.

The D value derived from IVIM reflects pure molecular diffusion, because it minimizes the influence of blood flow on tissue diffusion. The aggravation of DKD architectural malformation and the increased cell density destroy the microcirculation and affect the diffusion of water which restricts water molecule movement in turn exhibits a lower D value [37, 38]. Several studies have shown that IVIM is sensitive to renal dysfunction, renal artery stenosis, allograft rejection, and the early changes in DKD [39]. Although the D value decreased with renal dysfunction and predicted a poor outcome in current study (AUC = 0.77), we supposed that the combination of R2* and D may improve the efficiency of prediction. Our results demonstrated both MR2* and CD strongly correlated with the outcomes of DKD. It is noteworthy that the combination of MR2* and CD was more significant than each single value (Fig. 3f) to predict the prognosis.

The potential pernicious influence of etiology diversity on the MRI detectable values in kidney was decreased, for all the patients were confined in a scope of DM patients; and consequently, the homogeneity of disease made the comparison valid. We found that the correlation of poor outcomes of DKD with basic fMRI values was confined not only in the cortex but also the medulla. Previous studies

reported that oxygenation in cortex other in medulla decreased in CKD [11, 24], because the reduction of blood flow in cortex [25] impacted on eGFR decline more than that in medulla [11]. However, renal medulla was relative hypoxic and more vulnerable to hypoxia compared to cortex as found in our results.

In our study, all patients were screened within average age of about 50-year-old and 10-year DM-duration, which were matched to non-DKD controls. To diminish the impact of long time observation for DKD, 35 of 77 patients at stage of CKD 3–4 were chosen; it enables us to observe the end point in relative short time. The age-, DM duration- and gender matched controls made the data comparable. Although a study displayed the positive relationship between R2* values and age [40, 41], our age- and gender- adjusted multivariable analysis (Table 1) proved R2* and D values were significantly associated with outcomes of DKD. We did not reveal that the correlations of age, ACR and the DM duration with the clinical outcomes of DKD, the underlying reasons might be the strict inclusive criteria and relative short follow-up time.

The perspective strengths of present study are the prospective cohort design, strict inclusive criteria, and the use of a well-validated protocol including reproducible analysis method of fMRI. To reduce the influence of hydration status on the BOLD signal [42], all the participants were asked to stop taking diuretics a day in advance, fasting and water-deprivation were conducted 6 hours before the examination. To avoid a system bias, we applied a validated TLCO technique, which integrates geometrical information and takes into account the entire renal parenchyma. The intervening measure mentioned above made it more sensitive to identify the differences than the partial harvested data and shows excellent reproducibility and lower variability.

A limitation of current study is that a relative high percentage of advanced DKD enrolled. It shortens the time for observation, but the complications coming up with advanced DKD decreased the validation of current conclusions. Then, we did not have the histologic “gold standard” for all the participants to validate MRI data, although renal biopsy was also limited in predicting the decline of renal function in DKD. Last, we did not monitor the level of hypoxia and fibrosis by a second- or a third-time MRI, which would enable us to evaluate whether the long-term changes in kidney were consistent with the development of DKD.

In summary, this study describes the prediction value of fMRI in the assessment of DKD prognosis. Although fMRI is so far largely restricted in the research setting, our study indeed demonstrates that the values derived from fMRI correspond to hypoxemia and fibrosis in kidney, consequently, project the outcomes of DKD.

Conclusion

Integrating BOLD and IVIM-DWI improves the efficiency of assessment, and can be an increasingly accepted potential tool to predict the prognosis of DKD in clinical practice.

Abbreviations

ACR:albumin-creatinine ratio; ADC:apparent diffusion coefficient; AUC:area under the curve; BOLD:blood oxygen level-dependent; CD:cortical D value; CKD-EPI:Chronic Kidney Disease Epidemiology Collaboration; DKD:diabetic kidney disease; DM:diabetes mellitus; DWI:diffusion-weighted image; ECT-GFR:emission computed tomography-measured GFR; eGFR:estimated glomerular filtration rate; ESRD:end-stage renal disease; fMRI:functional magnetic resonance imaging; Hb:hemoglobin; IQR:interquartile range; IVIM:intravoxel incoherent motion; MR2*:medullary R2* value; MRI:magnetic resonance imaging; ROC:receiver-operating characteristic; Scr:serum creatinine.

Declarations

Ethics approval and consent to participate

This project was approved by the medical ethics committee of Guangdong General Hospital, Guangdong Academy of Medical Sciences (ID: No.GDREC2017253H), and conducted according to the principles of the Declaration of Helsinki. The written informed consent was obtained from each participant prior to data collection.

Consent for publication

Not applicable.

Competing interests

The authors declare that they have no competing interests.

Funding

This work was supported by the grants from National Natural Science Foundation of China (NO. 81270816 & NO. 81470974 to W.J.W), and High-level Hospital Construction Project of Guangdong Province (DFJH201908 to W.J.W).

Authors’ contributions

WJ.Wang and SX.Zhang conceived of the study. XL.Liang, J.Kuang, ZW.Li, HM.Chen and ZY.Liu participated in its design, coordination and developed the protocol. ZY.Liu and SX.Zhang developed the well-validated, reproducible method called twelve-layer concentric objects (TLCO). J.Li, XK.Mo and YH.Wang performed MRI processing and data acquisition. L.Zhang, T.Lin, RZ.Li, ZL.Li, S.Li and ST.Zhang followed up the patients. QL.Li, CF.Qi, TT.Liang, YF.Zhang, SG.Zhang, ZJ.Chen, XQ.Qiu, SC.Lin and J.Li

collected the data and performed statistics analysis. J.L, JT.X, and WJ.W edited all tables, prepared all figures and drafted the manuscript. All authors read and approved the final manuscript.

Acknowledgments

Sincere gratitude was expressed to the patients who participated in this study.

References

1. Thomas MC, Brownlee M, Susztak K, Sharma K, Jandeleit-Dahm KA, Zoungas S, Rossing P, Groop PH, Cooper ME. Diabetic kidney disease. Nat Rev Dis Primers 2015, 1:15018.
2. Jha V, Garcia-Garcia G, Iseki K, Li Z, Naicker S, Plattner B, Saran R, Wang AY, Yang CW. Chronic kidney disease: global dimension and perspectives. Lancet 2013, 382(9888):260–272.
3. Coresh J, Selvin E, Stevens LA, Manzi J, Kusek JW, Eggers P, Van Lente F, Levey AS. Prevalence of chronic kidney disease in the United States. JAMA 2007, 298(17):2038–2047.
4. Introduction: The American Diabetes Association's (ADA) evidence-based practice guidelines, standards, and related recommendations and documents for diabetes care. Diabetes Care 2012, 35 Suppl 1:S1-2.
5. Pruijm M, Mendichovszky IA, Liss P, Van der Niepen P, Textor SC, Lerman LO, Krediet CTP, Caroli A, Burnier M, Prasad PV. Renal blood oxygenation level-dependent magnetic resonance imaging to measure renal tissue oxygenation: a statement paper and systematic review. Nephrol Dial Transplant 2018, 33(suppl_2):ii22-ii28.
6. Chang D, Wang YC, Xu TT, Peng XG, Cai Y, Wang L, Bai YY, Ju S. Noninvasive Identification of Renal Hypoxia in Experimental Myocardial Infarctions of Different Sizes by Using BOLD MR Imaging in a Mouse Model. Radiology 2018, 286(1):129–139.
7. Manotham K, Tanaka T, Matsumoto M, Ohse T, Miyata T, Inagi R, Kurokawa K, Fujita T, Nangaku M. Evidence of tubular hypoxia in the early phase in the remnant kidney model. J Am Soc Nephrol 2004, 15(5):1277–1288.
8. Pedersen M, Dissing TH, Morkenborg J, Stodkilde-Jorgensen H, Hansen LH, Pedersen LB, Grenier N, Frokiaer J. Validation of quantitative BOLD MRI measurements in kidney: application to unilateral ureteral obstruction. Kidney Int 2005, 67(6):2305–2312.
9. Yin WJ, Liu F, Li XM, Yang L, Zhao S, Huang ZX, Huang YQ, Liu RB. Noninvasive evaluation of renal oxygenation in diabetic nephropathy by BOLD-MRI. Eur J Radiol 2012, 81(7):1426–1431.
10. Inoue T, Kozawa E, Okada H, Inukai K, Watanabe S, Kikuta T, Watanabe Y, Takenaka T, Katayama S, Tanaka J, et al. Noninvasive evaluation of kidney hypoxia and fibrosis using magnetic resonance imaging. J Am Soc Nephrol 2011, 22(8):1429–1434.
11. Pruijm M, Milani B, Pivin E, Podhajska A, Vogt B, Stuber M, Burnier M. Reduced cortical oxygenation predicts a progressive decline of renal function in patients with chronic kidney disease. Kidney Int

2018, 93(4):932–940.

12. Zhou H, Yang M, Jiang Z, Ding J, Di J, Cui L. Renal Hypoxia: An Important Prognostic Marker in Patients with Chronic Kidney Disease. Am J Nephrol 2018, 48(1):46–55.
13. Leung G, Kirpalani A, Szeto SG, Deeb M, Foltz W, Simmons CA, Yuen DA. Could MRI Be Used To Image Kidney Fibrosis? A Review of Recent Advances and Remaining Barriers. Clin J Am Soc Nephrol 2017, 12(6):1019–1028.
14. Caroli A, Schneider M, Friedli I, Ljimani A, De Seigneux S, Boor P, Gullapudi L, Kazmi I, Mendichovszky IA, Notohamiprodjo M, et al. Diffusion-weighted magnetic resonance imaging to assess diffuse renal pathology: a systematic review and statement paper. Nephrol Dial Transplant 2018, 33(suppl_2):ii29-ii40.
15. Togao O, Doi S, Kuro-o M, Masaki T, Yorioka N, Takahashi M. Assessment of renal fibrosis with diffusion-weighted MR imaging: study with murine model of unilateral ureteral obstruction. Radiology 2010, 255(3):772–780.
16. Thoeny HC, De Keyzer F, Oyen RH, Peeters RR. Diffusion-weighted MR imaging of kidneys in healthy volunteers and patients with parenchymal diseases: initial experience. Radiology 2005, 235(3):911–917.
17. Chandarana H, Lee VS, Hecht E, Taouli B, Sigmund EE. Comparison of biexponential and monoexponential model of diffusion weighted imaging in evaluation of renal lesions: preliminary experience. Invest Radiol 2011, 46(5):285–291.
18. Hennedige T, Koh TS, Hartono S, Yan YY, Song IC, Zheng L, Lee WS, Rumpel H, Martarello L, Khoo JB, et al. Intravoxel incoherent imaging of renal fibrosis induced in a murine model of unilateral ureteral obstruction. Magn Reson Imaging 2015, 33(10):1324–1328.
19. Ren T, Wen CL, Chen LH, Xie SS, Cheng Y, Fu YX, Oesingmann N, de Oliveira A, Zuo PL, Yin JZ, et al. Evaluation of renal allografts function early after transplantation using intravoxel incoherent motion and arterial spin labeling MRI. Magn Reson Imaging 2016, 34(7):908–914.
20. Yan YY, Hartono S, Hennedige T, Koh TS, Chan CM, Zhou L, Rumpel H, Martarello L, Khoo JB, Koh DM, et al. Intravoxel incoherent motion and diffusion tensor imaging of early renal fibrosis induced in a murine model of streptozotocin induced diabetes. Magn Reson Imaging 2017, 38:71–76.
21. Cai XR, Yu J, Zhou QC, Du B, Feng YZ, Liu XL. Use of intravoxel incoherent motion MRI to assess renal fibrosis in a rat model of unilateral ureteral obstruction. J Magn Reson Imaging 2016, 44(3):698–706.
22. Vermathen P, Binser T, Boesch C, Eisenberger U, Thoeny HC. Three-year follow-up of human transplanted kidneys by diffusion-weighted MRI and blood oxygenation level-dependent imaging. J Magn Reson Imaging 2012, 35(5):1133–1138.
23. National Kidney F. KDOQI Clinical Practice Guideline for Diabetes and CKD: 2012 Update. Am J Kidney Dis 2012, 60(5):850–886.
24. Milani B, Ansaloni A, Sousa-Guimaraes S, Vakilzadeh N, Piskunowicz M, Vogt B, Stuber M, Burnier M, Pruijm M. Reduction of cortical oxygenation in chronic kidney disease: evidence obtained with a new

analysis method of blood oxygenation level-dependent magnetic resonance imaging. Nephrol Dial Transplant 2017, 32(12):2097–2105.

25. Fine LG, Norman JT. Chronic hypoxia as a mechanism of progression of chronic kidney diseases: from hypothesis to novel therapeutics. Kidney Int 2008, 74(7):867–872.
26. Nangaku M. Chronic hypoxia and tubulointerstitial injury: a final common pathway to end-stage renal failure. J Am Soc Nephrol 2006, 17(1):17–25.
27. Haase VH. Mechanisms of hypoxia responses in renal tissue. J Am Soc Nephrol 2013, 24(4):537–541.
28. Mason RP. Non-invasive assessment of kidney oxygenation: a role for BOLD MRI. Kidney Int 2006, 70(1):10–11.
29. Beeman SC, Cullen-McEwen LA, Puelles VG, Zhang M, Wu T, Baldelomar EJ, Dowling J, Charlton JR, Forbes MS, Ng A, et al. MRI-based glomerular morphology and pathology in whole human kidneys. Am J Physiol Renal Physiol 2014, 306(11):F1381-1390.
30. Warner L, Glockner JF, Woollard J, Textor SC, Romero JC, Lerman LO. Determinations of renal cortical and medullary oxygenation using blood oxygen level-dependent magnetic resonance imaging and selective diuretics. Invest Radiol 2011, 46(1):41–47.
31. Li LP, Storey P, Pierchala L, Li W, Polzin J, Prasad P. Evaluation of the reproducibility of intrarenal R2* and DeltaR2* measurements following administration of furosemide and during waterload. J Magn Reson Imaging 2004, 19(5):610–616.
32. Gomez SI, Warner L, Haas JA, Bolterman RJ, Textor SC, Lerman LO, Romero JC. Increased hypoxia and reduced renal tubular response to furosemide detected by BOLD magnetic resonance imaging in swine renovascular hypertension. Am J Physiol Renal Physiol 2009, 297(4):F981-986.
33. Fine LG, Dharmakumar R. Limitations of BOLD-MRI for assessment of hypoxia in chronically diseased human kidneys. Kidney Int 2012, 82(8):934–935; author reply 935.
34. Neugarten J. Renal BOLD-MRI and assessment for renal hypoxia. Kidney Int 2012, 81(7):613–614.
35. Piskunowicz M, Hofmann L, Zuercher E, Bassi I, Milani B, Stuber M, Narkiewicz K, Vogt B, Burnier M, Pruijm M. A new technique with high reproducibility to estimate renal oxygenation using BOLD-MRI in chronic kidney disease. Magn Reson Imaging 2015, 33(3):253–261.
36. Pruijm M, Milani B, Burnier M. Blood Oxygenation Level-Dependent MRI to Assess Renal Oxygenation in Renal Diseases: Progresses and Challenges. Front Physiol 2016, 7:667.
37. Quaggin SE, Kapus A. Scar wars: mapping the fate of epithelial-mesenchymal-myofibroblast transition. Kidney Int 2011, 80(1):41–50.
38. Eddy AA. Overview of the cellular and molecular basis of kidney fibrosis. Kidney Int Suppl (2011) 2014, 4(1):2–8.
39. Deng Y, Yang B, Peng Y, Liu Z, Luo J, Du G. Use of intravoxel incoherent motion diffusion-weighted imaging to detect early changes in diabetic kidneys. Abdom Radiol (NY) 2018, 43(10):2728–2733.

40. Macisaac RJ, Ekinci EI, Jerums G. Markers of and risk factors for the development and progression of diabetic kidney disease. Am J Kidney Dis 2014, 63(2 Suppl 2):S39-62.
41. Simon-Zoula SC, Hofmann L, Giger A, Vogt B, Vock P, Frey FJ, Boesch C. Non-invasive monitoring of renal oxygenation using BOLD-MRI: a reproducibility study. NMR Biomed 2006, 19(1):84–89.
42. Pruijm M, Hofmann L, Piskunowicz M, Muller ME, Zweiacker C, Bassi I, Vogt B, Stuber M, Burnier M. Determinants of renal tissue oxygenation as measured with BOLD-MRI in chronic kidney disease and hypertension in humans. PLoS One 2014, 9(4):e95895.

Figures

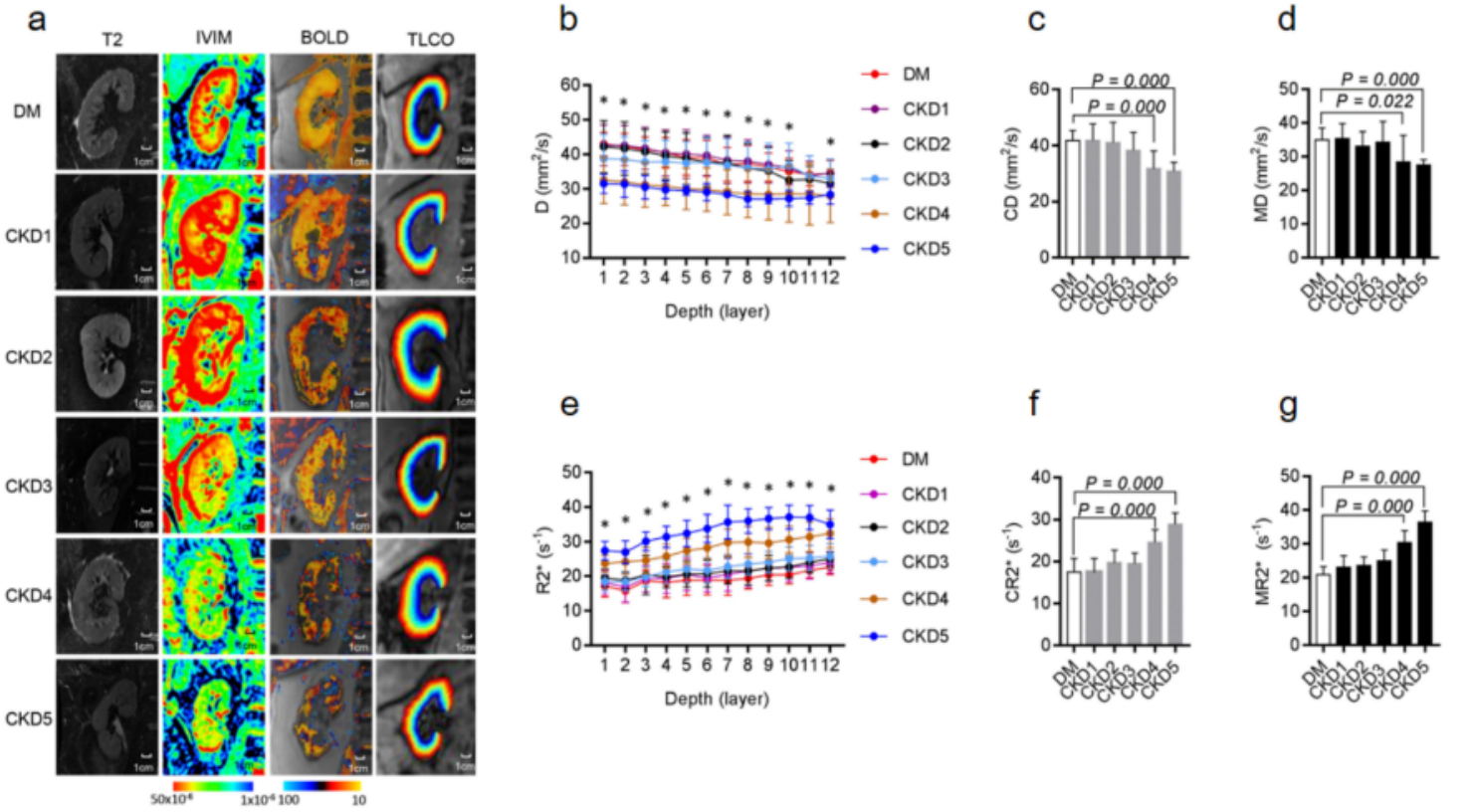

Figure 1

Pseudo-color maps and graphic depictions based on CKD stage. (a) Imaging characteristic of BOLD and IVIM obtained from patients at different stages of renal function. T2 imaging only detect the morphologic changes of the kidney; IVIM detected the diffusion of water declined as the disease aggravated. BOLD detected the change of the oxygenation; TLCO divides the renal parenchyma into 12 layers of equal thickness. (b) D profiles of CKD and DM. Comparison of CD (c) and MD (d) of patients at CKD stage 1-5 with DM. (e) R2* profiles of CKD and DM. Comparison of CR2* (f) and MR2*(g) of patients at CKD stage 1-5 with DM. One-way ANOVA test was used for the difference of fMRI values between CKD and DM, *P<0.05. BOLD, blood oxygen level dependent image; CD, cortical D value; CKD, chronic kidney disease;

CR2*, cortical R2* value; DM, diabetes mellitus; IVIM, intravoxel incoherent motion; MD, medullary D value; MR2*, medullary R2* value; TLCO, twelve-layer concentric objects; T2: T2-weighted imaging.

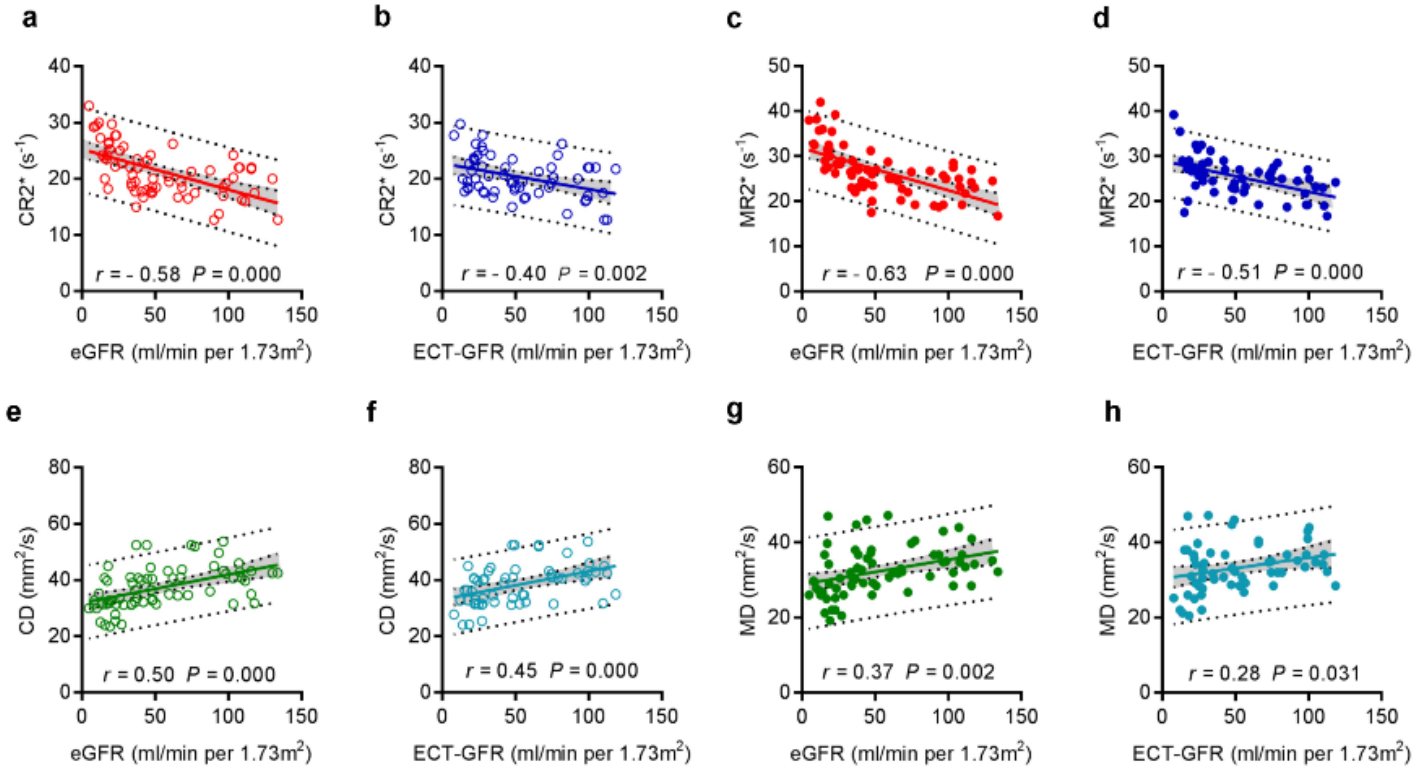

Figure 2

Correlations of MRI values with renal function. All R2* values negatively correlated with both eGFR (a, c) and ECT-GFR (b, d). Correlation of MR2* with eGFR (c) exhibited priority to others by its higher r. All D values positively correlated with both eGFR (e, g) and ECT-GFR (f, h). Correlation of CD with eGFR (e) exhibited priority to others by its higher r. All significant correlations are given as Pearson's r, P<0.05. The grey area represents the 95% confidence interval. CD, cortical D value; CR2*, cortical R2* value; ECT-GFR, emission computed tomography-glomerular filtration rate; eGFR, estimated glomerular filtration rate; MD, medullary D value; MR2*, medullary R2* value.

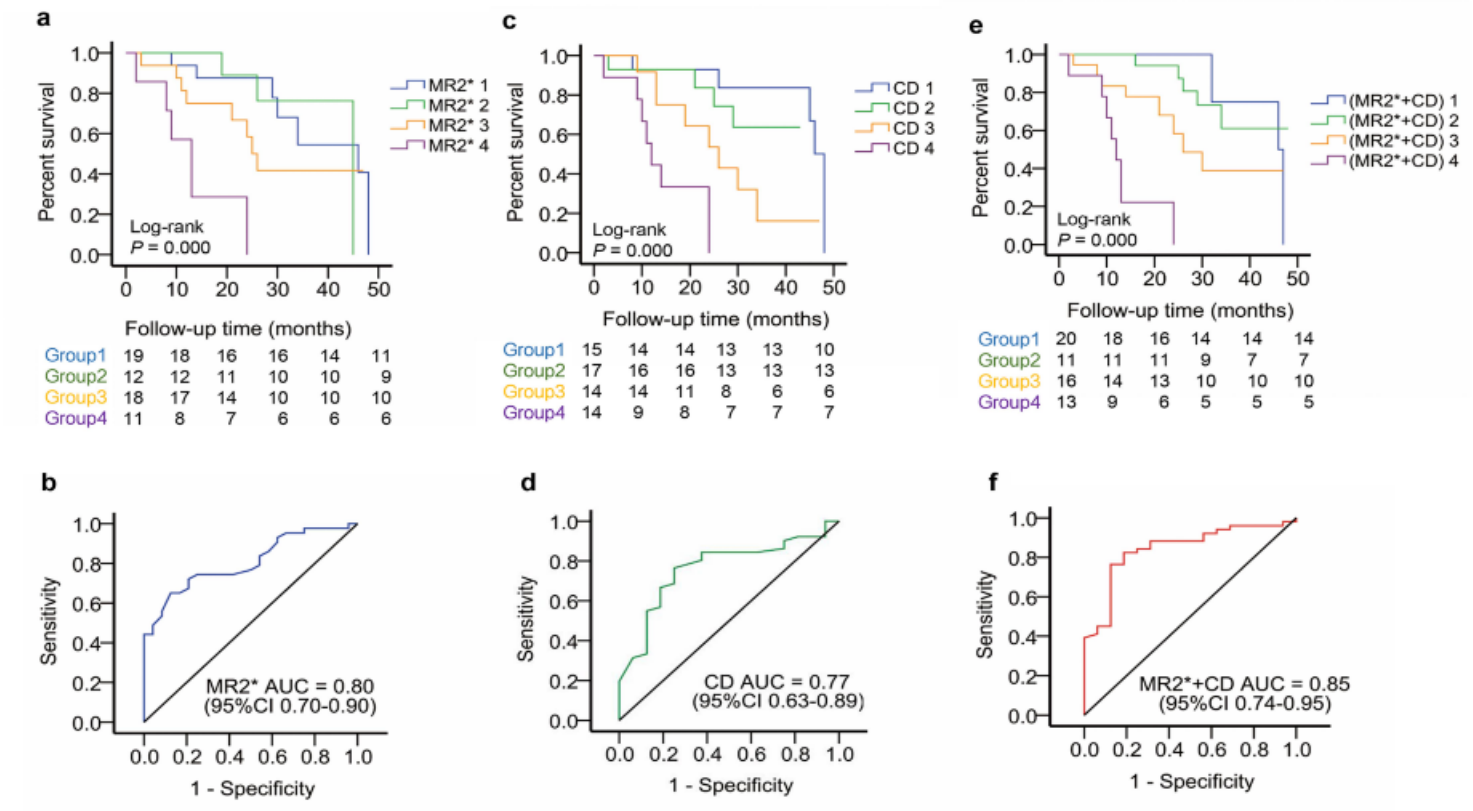

Figure 3

Kaplan-Meier curves and ROC curves of MR2* and CD values for their prediction of outcomes in CKD patients. (a) Kaplan-Meier curve of the patients grouped according to the IQR of MR2*. (b) ROC curves and corresponding AUC of MR2*values. (c) Kaplan-Meier curve of the patients grouped according to the IQR of CD values. (d) ROC curves and corresponding AUC of CD. (e) Kaplan-Meier curve of the patients grouped according to the IQR of MR2* and CD combination. (f) ROC curves and corresponding AUC of MR2* and CD combination. Log-rank test used for the statistical significance among the groups, P<0.05. AUC, area under the curve; CD, cortical D value; IQR, interquartile range; MR2*, medullary R2* value; ROC, receiver operating characteristic.

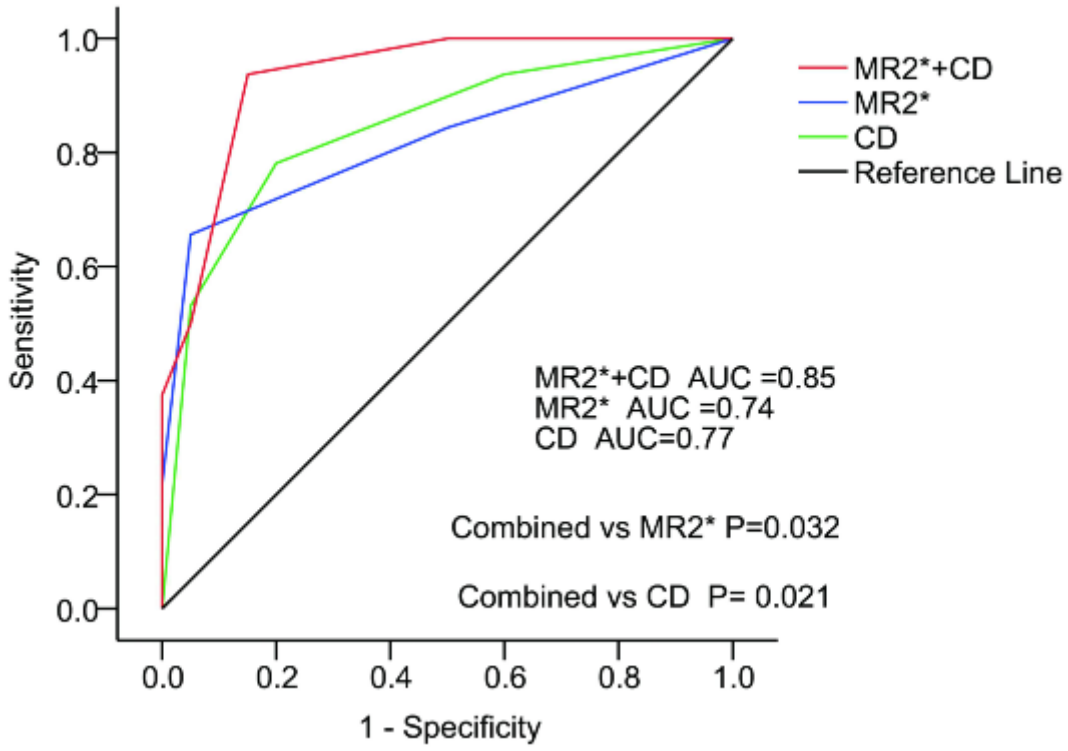

Figure 4

Comparison of the AUCs of CD (in green), MR2* (in blue), and the combination of CD and MR2* (in red) for their prediction of the outcomes of DKD. AUC, area under the curve; CD, cortical D value; DKD, diabetic kidney disease; MR2*, medullary R2* value; ROC, receiver operating characteristic

Supplementary Files

This is a list of supplementary files associated with this preprint. Click to download.

- Supplementarytitlesandlegends.docx
- SupplementalTable1.doc
- SupplementalTable2.docx
- SupplementalTable3.docx
- SupplementalTable4.docx
- SupplementalTable5.docx
- SupplementalTable6.docx
- Supplementalfigure1.jpg
- Supplementalfigure2.jpg